Dalton Transactions

Cite this: *Dalton Trans.*, 2011, **40**, 8675

www.rsc.org/dalton

PAPER

Interaction of Co(II), Ni(II) and Cu(II) with dibenzo-substituted macrocyclic ligands incorporating both symmetrically and unsymmetrically arranged N, O and S donors†

I. M. Vasilescu,[a] D. S. Baldwin,[a] D. J. Bourne,[b] J. K. Clegg,[c] F. Li,[c] L. F. Lindoy*[c] and G. V. Meehan*[a]

Received 28th March 2011, Accepted 9th June 2011
DOI: 10.1039/c1dt10523j

The synthesis and characterisation of four 17-membered, dibenzo-substituted macrocyclic ligands incorporating unsymmetrical arrangements of their N_3S_2, N_3O_2 and N_3OS (two ligands) donor atoms are described; these rings complete the matrix of related macrocyclic systems incorporating both symmetric and unsymmetric donor sets reported previously. The X-ray structures of three of the new macrocycles are reported. In two of the Cu(II) structures only three of the possible five donor atoms present in the corresponding macrocyclic ligand bind to the Cu(II) site, whereas all five donors are coordinated in each of the remaining complexes. The interaction of Co(II), Ni(II) and Cu(II) with the unsymmetric macrocycle series has been investigated by potentiometric (pH) titration in 95% methanol; X-ray structures of two nickel and three copper complexes of these ligands, each exhibiting 1 : 1 (M : L) ratios, have been obtained. The results are discussed in the context of previous results for these metals with the analogous 17-membered ring systems incorporating symmetrical arrangements of their donor atoms, with emphasis being given to both the influence of the donor atom set, as well as the donor atom sequence, on the nature of the resulting complexes.

Introduction

Over recent years there has been increased interest in the synthesis of unsymmetrical ligands and their potential for use in a number of applications.[1–6] For example, ligands of this type have been investigated in catalysis,[7] liquid crystal[8] and non-linear optics applications.[1]

We now report the results of a comparative investigation of the interaction of the 17-membered, unsymmetrical, mixed-donor macrocycles **1–9** (see Scheme 1) with Co(II), Ni(II) and Cu(II). In earlier studies we have reported the use of the corresponding 16- to 20-membered symmetrical macrocycles (the 17-membered rings are given by **10–18**; see Scheme 1) for the systematic investigation of metal ion discrimination behaviour across the industrially important metal ions: Co(II), Ni(II), Cu(II), Zn(II), Cd(II), Ag(I) and Pb(II).[9–10] In these studies the effect of systematic variation of the donor atom set, the macrocyclic ring size and the addition of substituents to the macrocyclic ring were all employed as a means of enhancing selectivity for particular transition and post-transition metal ions of interest. The present investigation represents an extension of these prior studies in which aspects of the complexation behaviour of Co(II), Ni(II) and Cu(II) involving both the 17-membered unsymmetrical (**1–9**) and symmetrical (**10–18**) ligand series are compared.

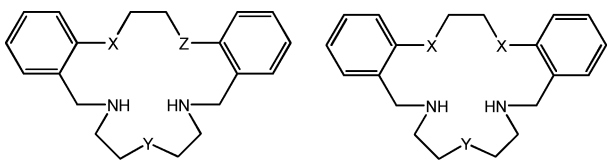

1 (SO/NNN); X = S, Z = O, Y = NH
2 (SO/NON); X = S, Z = O, Y = O
3 (SO/NSN); X = S, Z = O, Y = S
4 (SN/NNN); X = S, Z = NH, Y = NH
5 (SN/NON); X = S, Z = NH, Y = O
6 (SN/NSN); X = S, Z = NH, Y = S
7 (ON/NNN); X = O, Z = NH, Y = NH
8 (ON/NON); X = O, Z = NH, Y = S
9 (ON/NSN); X = O, Z = NH, Y = S

10 (NN/NNN); X = NH, Y = NH
11 (NN/NON); X = NH, Y = O
12 (NN/NSN); X = NH, Y = S
13 (OO/NNN); X = O, Y = NH
14 (OO/NON); X = O, Y = O
15 (OO/NSN); X = O, Y = S
16 (SS/NNN); X = S, Y = NH
17 (SS/NON); X = S, Y = O
18 (SS/NSN); X = S, Y = S

Scheme 1 Structures of the 17-membered, unsymmetrical and symmetrical, mixed-donor macrocycles **1–18**; donor sets are shown in parenthesis.

Experimental

General

Unless otherwise specified reagents used for the syntheses were of the highest grade obtainable commercially. Di(2-aminoethyl)sulfide was prepared *via* a modification of

[a]*School of Pharmacy and Molecular Sciences, James Cook University, Townsville, Q 4814, Australia*
[b]*Defence Science and Technology Organisation, Melbourne, Vic 3207, Australia*
[c]*School of Chemistry, University of Sydney, NSW 2006, Australia. E-mail: lindoy@chem.usyd.edu.au*

† CCDC reference numbers 819258–819265. For crystallographic data in CIF or other electronic format see DOI: 10.1039/c1dt10523j

the previously reported preparation of (2-aminoethyl, 3-aminopropyl)sulfide.[11] Dichloromethane (DCM) was distilled from calcium hydride. *N*-(2-Aminoethyl)-1,3-propanediamine was dried over 4 Å molecular sieves prior to use. The macrocycle precursor dialdehydes 2-(2-(2-formylphenoxy)ethylthio)-benzaldehyde, 2-(2-(2-formylphenylamino)ethylthio)benzaldehyde and 2-(2-(2-formylphenoxy)ethylamino)benzaldehyde incorporating SO-, SN- and ON-donor sequences were prepared as described previously.[12] Samples for elemental analysis were dried over silica gel in a vacuum. Crystals were used directly for the X-ray diffraction studies after removal from the crystallisation solution.

Physical methods

^{1}H and ^{13}C NMR spectra were recorded using a Bruker AM-300 spectrometer. In cases where NH or OH proton signals were not clearly observed, they are omitted from the reported spectral assignment. Electrospray (FTICR-MS) for **5, 6, 8** and **9** were obtained on a Bruker BioApex 47e spectrometer. For the metal complexes positive ion ESI-HRMS mass spectra were recorded on samples dissolved in acetonitrile and analysed using a Bruker Apex Ultra Qe mass spectrometer with a 9.4 T magnet and a Bruker Electrospray Ion source. Accurate mass determination was carried out after external calibration using Agilent ESI-L tuning mix.

Macrocycle synthesis

Macrocycle 5 (SN/NON). Di(2-aminoethyl)ether dihydrochloride (0.363 g, 0.002 mol) was dissolved in warm absolute ethanol (200 mL) containing NaOH (0.2 g, 0.005 mol) and this solution was slowly added (10 h) under dry N_2 to 2-(2-(2-formylphenylamino)ethylthio)benzaldehyde (0.570 g, 0.002 mol) in warm absolute ethanol (500 mL). The mixture was refluxed for 2 h after which additional di(2-aminoethyl)ether dihydrochloride (0.05 g) was added followed after 1 h by addition of $NaBH_4$ (3.0 g, 0.081 mol) in small portions; refluxing was continued for an additional 3 h. The ethanol was removed under vacuum and the resulting crude product was partitioned between DCM (100 mL) and 1 M NaOH (100 mL). The layers were separated and the aqueous phase was extracted with DCM (2 × 100 mL). The combined organic layers were back-washed with water (100 mL) and then washed with saturated NaCl solution (200 mL). The organic solution was filtered and the DCM removed to yield a pale brown oil. Flash column chromatography on silica gel with 20% methanol in DCM as eluent followed by recrystallisation from acetonitrile afforded **5** as a white crystalline solid (0.380 g, 53%) (Found: C, 66.99; H, 7.66; N, 11.79; S, 8.71%. $C_{20}H_{27}N_3OS$ requires C, 67.19; H, 7.61; N, 11.75; S, 8.96%). ^{1}H NMR ($CDCl_3$) δ 2.79, br t, J = 4.8 Hz, 2H; 2.84, br t, J = 4.5 Hz, 2H; 3.39, m, 2H; 3.55, m, 2H; 3.57, m, 2H; 3.68, m, 2H; 3.85, s, 2H; 3.88, s, 2H; 6.63, d, J = 7.8 Hz, 1H, Ar; 6.66, m, 1H, Ar; 7.03, br d, J = 7.5 Hz, 1H, Ar; 7.11, m, 1H, Ar; 7.18, dt, J = 1.5, 7.8 Hz, 1H, Ar; 7.24, m, 1H, Ar; 7.25, m, 1H, Ar; 7.26, m, 1H, Ar. ^{13}C NMR ($CDCl_3$) δ 31.2, 40.9, 47.7, 48.7, 52.6, 53.7, 69.40, 69.45, 110.0, 116.5, 123.9, 124.86, 124.94, 128.1, 128.5, 129.9, 130.9, 136.1, 136.7, 147.6.

Macrocycle 6 (SN/NSN). Di(2-aminoethyl)sulfide (0.225 g, 0.0022 mol) in methanol (150 mL) was added dropwise over several hours to 2-(2-(2-formylphenylamino)ethylthio)benzaldehyde (0.335 g, 0.0012 mol) in refluxing methanol (250 mL). After 1 h, $NaBH_4$ (1.0 g, 0.027 mol) was added in small portions and refluxing was continued for an additional 3 h. The solvent was removed under vacuum and the residue was partitioned between aqueous 1 M NaOH (100 mL) and DCM (100 mL). The organic phase was removed and the aqueous layer was extracted with DCM (2 × 100 mL). The combined DCM extracts were then washed with water (50 mL) followed by saturated NaCl (100 mL). Filtration and removal of the solvent afforded the crude product as an orange–brown glass. Chromatography on silica gel with 2% methanol in DCM as eluent, followed by recrystallisation from a mixture of DCM/hexane/Et_2O yielded **6** as off-white crystals (0.370 g, 82%) (Found: C, 64.08; H, 7.23; N, 11.25; S, 17.29%. $C_{20}H_{27}N_3S_2$ requires C, 64.30; H, 7.28; N, 11.25; S, 17.17%). ^{1}H NMR ($CDCl_3$) δ 2.77, m, 2H; 2.79, m, 2H; 2.82, m, 2H; 2.86, m, 2H; 3.38, m, 2H; 3.56, m, 2H; 3.78, s, 2H; 3.92, s, 2H; 6.64, dt, J = 1.1, 7.4 Hz, 1H, Ar; 6.65, dd, J = 1.1, 8.0 Hz, 1H, Ar; 7.02, dd, J = 1.7, 7.5 Hz, 1H, Ar; 7.13, dt, J = 1.2, 7.4 Hz, 1H, Ar; 7.19, dt, J = 1.6, 7.7 Hz, 1H, Ar; 7.23, dt, J = 1.6, 7.9 Hz, 1H, Ar; 7.28, br d, J = 7.4 Hz, 1H, Ar; 7.31, br d, J = 7.9 Hz, 1H, Ar. ^{13}C NMR ($CDCl_3$) δ 32.4, 32.4, 32.7, 41.8, 46.8, 47.6, 52.4, 53.4, 110.0, 116.5, 123.8, 125.3, 126.5, 128.2, 128.6, 129.8, 130.7, 136.4, 137.3, 147.6.

Macrocycle 8 (ON/NON). Di(2-aminoethyl)ether dihydrochloride (0.366 g, 0.002 mol) in absolute ethanol (150 mL) was added dropwise over several hours to 2-(2-(2-formylphenoxy)ethylamino)benzaldehyde (0.536 g, 0.002 mol) in refluxing absolute ethanol (500 mL). After 8 h, $NaBH_4$ (2.0 g) was added in small portions and refluxing was continued for 6 h, followed by the addition of further $NaBH_4$ (1.0 g); the reaction mixture was heated at reflux for a further 8 h. The ethanol was removed under vacuum and the crude product was partitioned between DCM (100 mL) and 1 M aqueous NaOH solution (100 mL). The layers were separated and the aqueous phase was extracted with DCM (2 × 100 mL). The combined organic layers were back-washed with water (100 mL) and then washed with saturated aqueous NaCl (200 mL). The DCM solution was filtered and the DCM removed under vacuum to yield an off-white glass. Chromatography of this product on silica gel with methanol (5–20%) in DCM afforded **8** which was recrystallised from acetonitrile/methanol (1 : 1) mixture as a white crystalline solid (0.610 g, 88%) (Found: C, 70.42; H, 8.25; N, 12.26%. $C_{20}H_{27}N_3O_2$ requires C, 70.35; H, 7.97; N, 12.31%). ^{1}H NMR ($CDCl_3$) δ 2.72, br t, J = 4.8 Hz, 2H; 2.77, br t, J 4.8 Hz, 2H; 3.41, br t, J = 4.8 Hz, 2H; 3.57, br t, J = 4.5 Hz, 2H; 3.61, br t, J = 4.9 Hz, 2H; 3.81, s, 2H; 3.84, s, 2H; 4.29, br t, J = 4.5 Hz, 2H; 6.66, br d, J = 7.8 Hz, 1H, Ar; 6.67, m, 1H, Ar; 6.92, dt, J = 1.2, 6.9 Hz, 1H, Ar; 6.93, br d, J = 7.8 Hz, 1H, Ar; 7.05, dd, J = 1.4, 7.8 Hz, 1H, Ar; 7.21, m, 1H, Ar; 7.22, m, 1H, Ar; 7.23, m, 1H, Ar. ^{13}C NMR ($CDCl_3$) δ 43.2, 47.1, 48.6, 50.5, 53.8, 67.3, 68.9, 69.9, 109.8, 111.2, 116.4, 120.4, 124.3, 128.2, 128.38, 128.44, 129.7, 130.8, 147.9, 157.4.

Macrocycle 9 (ON/NSN). Di(2-aminoethyl)sulfide (0.320 g, 0.0026 mol) in absolute ethanol (250 mL) was added dropwise over several hours to 2-(2-(2- formylphenoxy)ethylamino)benzaldehyde (0.545 g, 0.009 mol) in refluxing absolute ethanol (500 mL) under nitrogen. Refluxing was continued overnight, $NaBH_4$ (2.50 g,

0.068 mol) was added in small portions and refluxing was continued for 12 h. After a further addition of $NaBH_4$ (1.0 g, 0.027 mol), the solution was refluxed for a further 4 h. The ethanol was removed under vacuum and the crude product was partitioned between DCM (100 mL) and aqueous 1 M NaOH (100 mL). The layers were separated and the aqueous phase was extracted with DCM (2 × 100 mL). The combined organic extracts were back-washed with water (100 mL) and then washed with saturated NaCl solution (200 mL). The solution was filtered and the DCM removed to yield a light-brown glass. Chromatography on silica gel with methanol (5–50%) in DCM as eluent resulted in **9** (0.321 g, 45%) as an off-white solid which was recrystallised from acetonitrile (Found: C, 66.87; 66.73; H, 7.63; 7.65; N, 11.85; 11.85; S, 8.03; 8.31%. $C_{20}H_{27}N_3OS$ requires C, 67.19; H, 7.61; N, 11.75; S, 8.96%). ^{1}H NMR ($CDCl_3$) δ 2.68–2.75, m, 4H; 2.88–2.95, m, 4H; 3.65, br t, J = 4.5 Hz, 2H; 3.74, s, 2H; 3.86, s, 2H; 4.26, br t, J = 4.5 Hz, 2H; 6.64, m, 1H, Ar; 6.66, br d, J = 8.1 Hz, 1H, Ar; 6.88, br d, J = 8.1 Hz, 1H, Ar; 6.90, br t, J 6.9 Hz, 1H, Ar; 7.04, br d, J = 7.2 Hz, 1H, Ar; 7.22, m, 3H, Ar. ^{13}C NMR ($CDCl_3$) δ 31.9, 32.3, 43.0, 47.0, 47.5, 49.5, 52.6, 66.6, 109.6, 111.1, 116.2, 120.6, 123.8, 126.6, 128.6, 128.9, 129.9, 130.6, 147.5, 157.3.

Synthesis of metal complexes

[NiLCl]Cl·3H$_2$O [L = 7 (ON/NNN)]. $NiCl_2·6H_2O$ (0.0179 g, 7.53×10^{-5} mol) in warm ethanol (10 mL) was added to **7** (0.025 g, 7.34×10^{-5} mol) in warm ethanol (20 mL) and the stirred solution was heated for 1 h then allowed to cool. Small green prisms of [Ni**L**Cl]Cl·3H_2O formed following diethyl ether vapour diffusion into the ethanol solution. Positive ion ESI-HRMS m/z detected as M^+ 433.13001 ($C_{20}H_{28}N_4OClNi$ requires 433.1296). A crystal from this synthesis was used for the X-ray structure determination.

[NiLCl]Cl·0.125CH$_3$CN·3.75H$_2$O [L = 8 (ON/NON)]. $NiCl_2·6H_2O$ (0.0191 g, 8.05×10^{-5} mol) was dissolved in warm ethanol (20 mL) and added to a warm solution of **8** (0.025 g, 7.32×10^{-5} mol) in ethanol (20 mL) with stirring. The reaction mixture was heated with stirring for 1 h. Several green, multi-faceted crystals of [Ni**L**Cl]Cl·0.125CH_3CN·3.75H_2O suitable for X-ray analysis were obtained following slow evaporation of the ethanol solution. Positive ion ESI-HRMS m/z detected as M^+ 434.11402 ($C_{20}H_{27}N_3O_2ClNi$ requires 434.11398). A crystal from this synthesis was used for the X-ray structure determination.

[CuLCl$_2$]·CH$_3$CN [L = 7 (ON/NNN)]. $CuCl_2·2H_2O$ (0.015 g, 8.79×10^{-5} mol) in warm acetonitrile (10 mL) was added to a warm solution of **7** (0.0199 g, 5.84×10^{-5} mol) in warm acetonitrile (15 mL) and the reaction mixture was stirred with low heat for 1 h. Green block-like crystals of [Cu**L**Cl$_2$]·CH_3CN (**L** = **7**) was obtained following slow diethyl ether vapour diffusion into the reaction solution. Positive ion ESI-HRMS m/z detected as [M – Cl^-]$^+$ 438.12385. ($C_{20}H_{28}N_4OClCu$ requires 438.12422). A crystal from this synthesis was used for the X-ray structure determination.

[CuLCl$_2$]·CH$_3$CN [L = 8 (ON/NSN)]. $CuCl_2·2H_2O$ (0.0138 g, 8.09×10^{-5} mol) in warm acetonitrile (5 mL) was added dropwise to a warm acetonitrile solution (20 mL) of **8** (0.0257, 7.53×10^{-5} mol). Several green, block-like crystals of [Cu**L**Cl$_2$]·CH_3CN suitable for X-ray crystallography study were obtained following slow diethyl ether diffusion into the acetonitrile solution. Positive ion ESI-HRMS m/z detected as [M – H_2, – Cl^-]$^+$ 437.09258 ($C_{20}H_{25}N_3O_2CuCl$ requires 437.09258). A crystal from this synthesis was used for the X-ray structure determination.

[CuLCl]Cl·2.375H$_2$O [L = 9 (ON/NSN)]. $CuCl_2·2H_2O$ (0.0138 g, 8.09×10^{-5} mol) in warm ethanol (5 mL) was added with stirring to an ethanol solution of **9** (0.0257 g, 7.32×10^{-5} mol) (20 mL). Small blue block-like crystals of [Cu**L**Cl]Cl·2.375H_2O were obtained following slow evaporation of the ethanol solution. Positive ion ESI-HRMS m/z detected as [(M – H_2)]$^+$ 453.07017 ($C_{20}H_{25}N_3OSCuCl$ requires 453.07047). A crystal from this synthesis was used for the X-ray structure determination.

Potentiometric titrations

The protonation constants and metal stability constants were determined by potentiometric (pH) titration. All measurements were performed in 95% methanol at 25 ± 0.1 °C (I = 0.1; NEt_4ClO_4) under the same conditions as described previously.[13] Metal complex log K values are the mean of between two and four individual determinations at varying metal : macrocycle ratios. The use of the above conditions allowed comparison of the data with values obtained for the previously reported macrocyclic analogues. Data were processed using a local version of MINIQUAD.[14]

Macrocycle X-ray Structures

The X-ray data for **5** (SN/NON), **6** (SN/NSN), **8** (ON/NON), [Ni**L**Cl]Cl·0.125CH_3CN·3.75H_2O [**L** = **8** (ON/NON)], [Cu**L**Cl$_2$]·CH_3CN [**L** = **7** (ON/NNN)], [Cu**L**Cl]Cl·2.375H_2O [**L** = **9** (ON/NSN)] and [Cu**L**Cl$_2$]·CH_3CN [**L** = **8** (ON/NON)] were collected on a Bruker-Nonius APEX2-X8-FR591 diffractometer employing graphite-monochromated Mo-Kα radiation generated from a rotating anode (0.71073 Å) with ω and ψ scans to approximately 56° 2θ at 150(2) K.[15] Data for [Ni**L**Cl]Cl·3H_2O [**L** = **7** (ON/NNN)] were collected with ω scans to approximately 56° 2θ using a Bruker SMART 1000 diffractometer employing graphite-monochromated Mo-Kα radiation generated from a sealed tube (0.71073 Å) at 150(2) K.[16] Data integration and reduction were undertaken with SAINT and XPREP[15–16] Subsequent computations were carried out using the WinGX-32 graphical user interface.[17] Structures were solved by direct methods using SIR97.[18] Multi-scan empirical absorption corrections, when used, were applied to the data sets using SADABS.[19] Data were refined and extended with SHELXL-97.[20] In general, non-hydrogen atoms with occupancies greater than 0.5 were refined anisotropically. Carbon-bound hydrogen atoms were included in idealised positions and refined using a riding model. Oxygen and nitrogen bound hydrogen atoms were first located in the difference Fourier map before refinement. Where these hydrogen atoms could not be located, they were not modelled. Crystallographic data are summarised in Table 1 and (additional) specific details pertaining to structural refinements for two complexes are detailed below.

[NiLCl]Cl·0.125CH$_3$CN·3.75H$_2$O [L = 8 (ON/NON)]. This molecule crystallises with two complexes in the asymmetric unit and there is a large amount of disordered solvent in the lattice. This was modelled as a quarter occupancy acetonitrile, two full

Table 1 Crystal and structure refinement data

Compound	**5** (SN/NON)	**6** (SN/NSN)	**8** (ON/NON)	[Cu**L**Cl$_2$]·CH$_3$CN [**L** = **7** (ON/NNN)]	[Ni**L**Cl]Cl·3H$_2$O [**L** = **7** (ON/NNN)]	[Ni**L**Cl]Cl·0.125CH$_3$CN·3.75H$_2$O [**L** = **8** (ON/NON)]	[Cu**L**Cl$_2$]·CH$_3$CN [**L** = **8** (ON/NON)]	[Cu**L**Cl]Cl·2.375H$_2$O [**L** = **9** (ON/NSN)]
Formula of refinement model	$C_{20}H_{27}N_3OS$	$C_{20}H_{27}N_3S_2$	$C_{20}H_{27}N_3O_2$	$C_{22}H_{31}Cl_2CuN_5O$	$C_{20}H_{34}Cl_2N_4NiO_4$	$C_{20.25}H_{34.875}Cl_2N_{3.125}NiO_{5.75}$	$C_{22}H_{30}Cl_2CuN_4O_2$	$C_{20}H_{28.125}Cl_2CuN_3O_{3.375}S$
Molecular weight	357.51	373.57	341.45	515.96	524.12	543.75	516.94	531.08
Crystal system	Triclinic	Triclinic	Triclinic	Monoclinic	Monoclinic	Monoclinic	Monoclinic	Monoclinic
Space group	$P\bar{1}$ (#2)	$P\bar{1}$ (#2)	$P\bar{1}$ (#2)	$C2/c$ (#15)	$C2/m$ (#14)	$P21/n$ (#14)	$P21/c$ (#14)	$C2/c$ (#15)
a/Å	8.9772(8)	9.4397(12)	9.1852(10)	21.9824(12)	16.696(2)	12.0787(8)	10.6290(6)	16.9284(17)
b/Å	11.2223(8)	10.8410(14)	10.0015(9)	8.3281(4)	15.556(2)	18.0874(13)	9.9320(5)	16.2096(17)
c/Å	11.6609(15)	11.552(2)	10.9234(8)	26.8453(15)	8.8940(12)	24.7617(18)	22.7210(13)	38.129(4)
α (°)	116.367(8)	104.996(13)	71.742(6)					
β (°)	110.079(9)	104.979(13)	86.090(7)	97.319(3)	90.522(2)	100.238(2)	90.271(5)	95.261(4)
γ (°)	94.316(6)	111.385(9)	73.961(8)					
V/Å^3	951.70(20)	978.1(3)	915.69(15)	4874.6(4)	2309.9(5)	5323.6(6)	2398.6(2)	10418.5(18)
D_c/g cm^{-1}	1.248	1.268	1.238	1.406	1.507	1.357	1.432	1.354
Z	2	2	2	8	4	8	4	16
Crystal size/mm	0.28 × 0.12 × 0.11	0.17 × 0.09 × 0.07	0.30 × 0.10 × 0.08	0.28 × 0.25 × 0.18	0.40 × 0.35 × 0.30	0.30 × 0.25 × 0.20	0.28 × 0.25 × 0.20	0.10 × 0.075 × 0.05
Crystal colour	colourless	colourless	colourless	green	green	green	green	blue
Crystal habit	shard	shard	shard	block	prism	multi-face	block	block
T/K	150(2)	150(2)	150(2)	150(2)	150(2)	150(2)	150(2)	150(2)
λ(Mo-Kα)/Å	0.71073	0.71073	0.71073	0.71073	0.71073	0.71073	0.71073	0.71073
μ(Mo-Kα)/mm^{-1}	0.183	0.28	0.081	1.139	1.106	0.966	1.159	1.149
T(SADABS)$_{min,max}$	0.826, 0.980	0.799, 0.981	0.801, 0.990	0.738, 0.815	0.6146, 0.7457	0.693, 0.824	0.6760, 0.7456	0.806, 0.944
$2\theta_{max}$ (°)	66.32	56.66	66.14	60.06	56.58	55.28	54.88	44.10
hkl range	–13 13, –17 17, –17 17	–12 12, –14 14, –15 15	–14 14, –15 14, –16 16	–30 30, –11 11, –37 37	–21 21, –20 19, –11 11	–15 13, –22 23, –32 27	–13 13, –12 12, –29 26	–17 17, –13 17, –31 40
N	45310	45395	36808	51326	11490	42018	26255	23228
N_{ind} (R_{merge})	7186 (0.0720)	4854 (0.0872)	6910(0.0554)	7111 (0.0428)	2854 (0.0223)	12334 (0.0337)	5463 (0.0284)	6334 (0.0316)
N_{obs} ($I > 2\sigma(I)$)	5719	4082	5032	5492	2677	8470	4938	5150
N_{var}	235	235	232	293	170	651	284	559
$R_1(F)$ (obs)	0.0539	0.0644	0.0604	0.0338	0.0320	0.0778	0.0241	0.0837
w$R_2(F^2)$ (all)	0.1234	0.1274	0.1730	0.0842	0.0876	0.2631	0.0932	0.2465
GoF	1.054	1.178	1.053	1.026	1.091	1.053	1.179	1.056
$\Delta\rho_{min,max}$/e$^-$ Å^{-3}	–0.375, 0.489	–0.289, 0.458	–0.456, 0.579	–0.323, 1.000	–0.500, 0.548	–1.396, 1.379	–0.680, 0.609	–0.716, 1.273

occupancy water molecules, one three-quarter occupancy water molecule, six half-occupancy water molecules and eight quarter occupancy water molecules. Hydrogen atoms could not be located on the water molecules of half or lower occupancy and were not included in the model. In addition the lattice chloride anions are modelled each over two positions of 0.8 and 0.2 occupancy. Each disordered chloride was modelled with identical thermal parameters.

[CuLCl]Cl·2.375H$_2$O [L = 9 (ON/NSN)]. These crystals were very small and despite appearing (at least visually) to be of good quality they were poorly diffracting, with few reflections recorded above 1 Å resolution. This complex crystallises with two molecules in the asymmetric unit and the uncoordinated anions and solvent water molecules are disordered. The 4.75 water molecules were modelled over 14 positions and their hydrogen atoms could not be located in the difference Fourier map. In addition, the uncoordinated chloride ions were modelled over eight positions. One of the coordinated chlorides (Cl(3)) was modelled over two (0.75 and 0.25 occupancy) positions. The O–N ethylene bridge in one of the macrocycles was modelled as disordered over two positions.

Results and discussion

Macrocycle synthesis and characterisation

The unsymmetrical 17-membered macrocycles **1** (SO/NNN), **2** (SO/NON), **3** (SO/NSN), **4** (SN/NNN) and **7** (ON/NNN) have been reported previously by our group[12] while the remainder of the series, **5** (SN/NON), **6** (SN/NSN), **8** (ON/NON) and **9** ON/NSN), are new and serve to complete the 'matrix' of 17-membered macrocyclic ligands of this type. The preparations in each case involved a double Schiff-base condensation between the appropriate linear diamine derivative and the corresponding unsymmetrical dialdehyde precursor, followed by *in situ* reduction of the resulting diimine with sodium borohydride. Isolation of the diimine (or its isomeric 1,3-diazacyclopentane)[21] intermediate prior to reduction was found to be unnecessary. The microanalytical, mass spectra, ^{1}H and ^{13}C NMR results were in each case in accord with formation of the expected product. Structural assignments were initially carried out with the aid of 1D and 2D NMR experiments and subsequently confirmed in three instances by single crystal X-ray analysis (see below).

The 1D and 2D NMR data for **5** (SN/NON), **6** (SN/NSN), **8** (ON/NON) and **9** (ON/NSN) are presented in Table 2 (see Fig. 1

Table 2 ^{1}H and ^{13}C NMR assignments (HSQC, J = 140 Hz) and long range correlations (HMBC, J = 8 Hz) for **5**, **6**, **8** and **9**

	5 (SN/NON)			**6** (SN/NSN)			**8** (ON/NON)			**9** (ON/NSN)		
C	δ^{13}C	δ^{1}H	HMBC Correlations	δ^{13}C	δ^{1}H	HMBC Correlations	δ^{13}C	δ^{1}H	HMBC Correlations	δ^{13}C	δ^{1}H	HMBC Correlations
1	136.7	—	—	137.3	—	—	128.2	—	—	126.6	—	—
2	136.1	—	—	136.4	—	—	157.4	—	—	157.3	—	—
3	—	—	—	126.5	7.31	C1	111.2	6.94	C2, C5	111.1	6.87	—
4	—	—	—	128.2	7.23	C2, C6	128.4[a]	7.23	—	128.6	7.20	C2
5	—	—	—	125.3	7.13	—	120.4	6.92	—	120.6	6.90	C3
6	130.9	7.26	—	130.7	7.28	C2, C4, C9	130.8	7.21	C2, C9	130.6	7.22	C9
1′	123.9	—	—	123.8	—	—	124.3	—	—	123.8	—	—
2′	129.9	7.03	—	129.8	7.02	C4′, C6′, C14	129.7	7.05	C4′, C6′, C14	129.9	7.04	C4′, C6′, C14
3′	—	—	—	116.5	6.64	—	116.4	6.67	C1′, C5′	116.2	6.64	C5′
4′	128.1	7.18	—	128.6	7.19	C2′, C6′	128.4[a]	7.21	—	128.8	7.23	C6′
5′	—	—	—	110.0	6.65	C1′	109.8	6.66	—′	109.6	6.68	C3′
6′	147.6	—	—	147.6	—	—	147.9	—	—	147.5	—	—
7	40.9	3.55	C8, C6′	41.8	3.56	C6′, C8	43.2	3.57	C6′, C8	43.0	3.65	C6′
8	31.2	3.39	C2, C7	32.4	3.38	C2, C7	67.3	4.29	C2, C7	66.6	4.26	C2, C7
9	52.6	3.88	C1, C2, C6, C10	52.4	3.92	C1, C2, C6, C10	50.5	3.84	C1, C2, C6, C10	49.5	3.86	C1, C2, C6, C10
10	47.7	2.84	C9, C11	46.8	2.82	—	47.1	2.72	C9, C11	47.0	2.91	—
11	69.5	3.68	—	32.4[a]	2.78	—	69.9	3.61	C10, C12	31.9[a]	2.72	—
12	69.4	3.57	—	32.6[a]	2.79	—	68.9	3.41	C11, C13	32.3[a]	2.72	—
13	48.7	2.79	C12, C14	47.6	2.86	C12	48.6	2.75	—	47.5	2.91	—
14	53.7	3.85	C1′, C2′, C6′, C13	53.4	3.78	C1′, C2′, C6′, C13	53.8	3.81	C1′, C2′, C6′, C13	52.6	3.74	C1′, C2′, C6′, C13

[a] Entries bearing this superscript are interchangeable

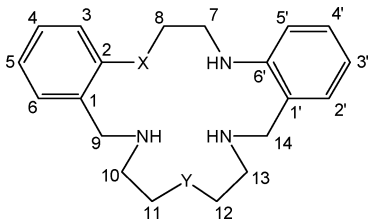

Fig. 1 The atom numbering scheme employed for the NMR assignments listed in Table 2.

for atom numbering); only the assignments for **5** (SN/NON) are discussed below – the corresponding assignments for **6** (SN/NSN), **8** (ON/NON) and **9** (ON/NSN) were made in an analogous manner. For **5**, the equivalence of the methylene hydrogens on each benzylic carbon (which appear as two-proton singlets at δ 3.88 (H9) and δ 3.85 (H14)) is in agreement with the expected conformational flexibility of the 'NON'-containing fragment of the macrocyclic ring. The respective long range proton–carbon correlations are also consistent with the proposed structure. Thus, the benzylic protons at δ 3.85 (H14) correlated across the nitrogen with the ethylene carbon in the lower bridge at δ 48.7 ppm (C13, adjacent to the secondary amine) and also to the aromatic carbon atoms at δ 123.9, 129.9 and 147.6 ppm (C1′, C2′ and C6′ respectively). These were assigned to the carbons of the N-substituted aromatic ring, using the low-field position at δ 147.6 ppm as evidence for N-substitution.[23] Similarly, the ethylene protons at δ 2.79 (H13, ethylene carbon at 48.7 ppm) in the 'NON' bridge showed correlations to the benzylic carbon at 53.7 ppm (C14) as well as to the carbon at 69.40 ppm (C12) adjacent to the ether oxygen in this bridge. For the opposite ('SN' bridge) side of the molecule, the connectivity was confirmed on the basis of correlations from the benzylic protons at δ 3.88 (H9) to the aromatic carbon signals at 130.9, 136.7, and 136.1 ppm (C6, C1 and C2 respectively) of the S-substituted ring. The assignment of the carbon at 136.1 ppm (C2) was made on the basis of a correlation from the upper bridge methylene protons at δ 3.39 (H8) and using the chemical shift of the carbon at the C8 position (31.2 ppm) as being diagnostic of attachment to sulfur.[22]

The X-ray structures of **5** (SN/NON), **6** (SN/NSN) and **8** (ON/NON) (see Fig. 2–4) in each case shows the presence of a non-folded conformation and confirm the atom connectivity deduced from the NMR experiments. The structures of **4** (SN/NNN), and **7** (ON/NNN), reported previously, also adopt quite related non-folded conformations.[12] In general, there is close agreement between bond lengths and angles of chemically equivalent bonds across all structures.

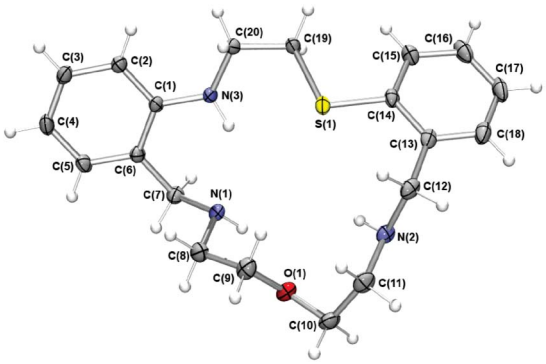

Fig. 2 The X-ray crystal structure of **5** (SN/NON). Hydrogen bond lengths and angles: N(2)–O(1) 2.9151(15) Å, 109.6(13)°; N(2)–S(1) 3.3770(12) Å, 120.0(13)°; N(3)–N(1) 2.8377(16) Å, 138.1(14)°; N(3)–S(1) 3.1530(10) Å, 109.2(12)°; N(1)–N(2)^{i} 3.1156(16) Å, 164.4(15)°. ^{i} –x +1, –y, –z +1.

Macrocycle **5** (SN/NON) was recrystallised from acetonitrile to yield colourless crystals suitable for diffraction studies. The crystal structure reveals an open arrangement of the macrocycle. The presence of secondary nitrogen atoms and five-hydrogen

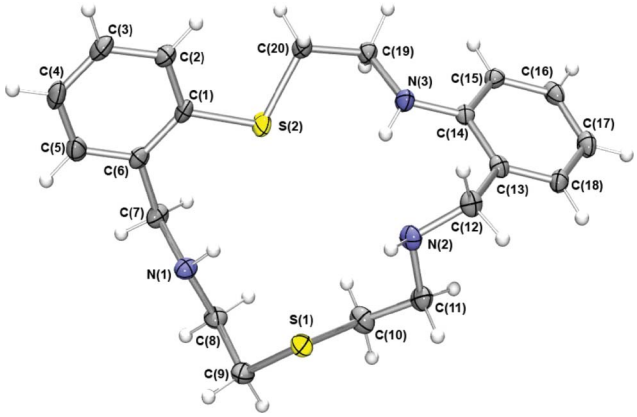

Fig. 3 The X-ray crystal structure of **7** (SN/NSN). Hydrogen bond lengths and angles: N(1)–S(2) 3.340(s) Å, 124(2)°; N(3)–N(2) 2.917(3) Å, 137(3)°.

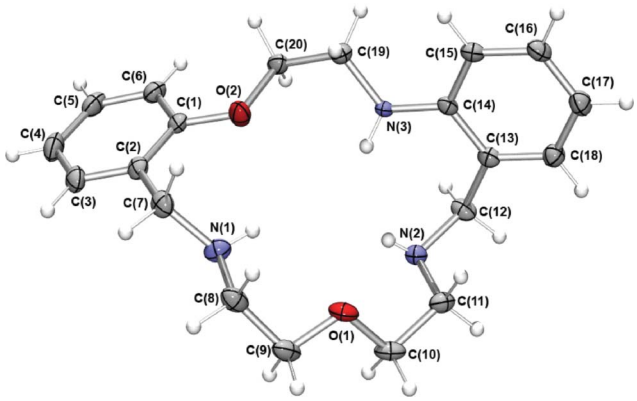

Fig. 4 The X-ray crystal structure of **9** (ON/NON). Hydrogen bond lengths and angles: N(1)–O(2) 2.9472(16) Å, 115.2(17)°; N(2)–O(1) 2.8976(16) Å, 111.5(19)°; N(2)–N(3) 3.0143(16) Å, 118.9(19)°; N(3)–N(2) 3.0143(16) Å, 127.5°.

bonding accepting groups (the three amines, the thioether and the ether) leads to the presence of a number of intramolecular hydrogen bonding interactions. N(2), for example, hydrogen bonds to both O(1) and S(1), while N(3) hydrogen bonds to N(1) and S(1). The remaining hydrogen bond donor (N(1)) is involved in intermolecular hydrogen bonding binding to the N(2) in an adjacent molecule forming a dimer-like arrangement. The crystal packing is further stabilised by a number of CH_2–π interactions.

In a similar fashion to **5** (SN/NON), just discussed, **6** (SN/NSN) crystallises in the triclinic space group $P\bar{1}$ and the molecule has significant potential for hydrogen bonding interactions. There are a number of intramolecular interactions present with N(1) hydrogen bonding to S(2) and N(3) to N(2). S(1) is not involved in these interactions, presumably because it is orientated such that its lone pairs point outside the macrocyclic cavity rather than internally. In contrast to the structure of **5** (SN/NON), there are no intermolecular hydrogen bonds present in the structure of **6**; however, there are a number of non-classical $CH_{phenylene}$–S interactions. The latter are associated with $CH_{phenylene}$–S(1) distances of ~3.0 Å.[23]

In a similar manner to both **5** (SN/NON) and **6** (SN/NSN), single colourless crystals of **8** (ON/NON) suitable for X-ray studies were obtained by recrystallisation from acetonitrile. In contrast to **7** (SN/NSN), but in a similar manner to **5** (SN/NON), the central donor (O(1) in this case) of the macrocyclic ring is orientated such that it faces into the centre of the 17-membered N_3O_2 macrocyclic ring. Once again there is extensive intramolecular hydrogen bonding present with each of the secondary amines acting as hydrogen-bond donors. N(1) hydrogen bonds to O(2) and N(3) to N(2), while N(2) interacts with both O(1) and N(3). There is a π–π interaction present between adjacent molecules indicated by a C(15)–C′(15) distance of 3.37 Å and a significant non-classical $CH_{phenylene}\cdots O$ interaction indicated by an C(16)H$\cdots$O(1) distance of 2.45 Å.[24]

Complex syntheses and X-ray studies

Reaction of individual ligands from **4–9** with selected metal salts in ethanol resulted in suitable crystals for X-ray diffraction in five instances; structure determinations were obtained for the following complexes: [Ni**L**Cl]Cl·3H_2O [**L** = **7** (ON/NNN)], [Ni**L**Cl]Cl·0.125CH_3CN·3.75H_2O [**L** = **8** (ON/NON)], [Cu**L**Cl_2]·CH_3CN [**L** = **7** (ON/NNN)], [Cu**L**Cl_2]·CH_3CN [**L** = **8** (ON/NON)] and [Cu**L**Cl]Cl·2.375H_2O [(**L** = **9** (ON/NSN)].

As occurs in the previously reported structures of the Ni(II) complexes of the related symmetrical **13** (OO/NNN),[25] **16** (SS/NNN)[26] and **18** (SS/NSN).[27] macrocycles, in both of the present nickel complexes the macrocycle binds to the metal centre by all five of its heteroatoms, with the –NYN– ligand fragment (Y = NH or S) arranged facially.

The chloro ligand in the complex cation of [Ni**L**Cl]Cl·3H_2O [**L** = **7** (ON/NNN)] occupies the sixth coordination site (Fig. 5). The observed distortion from regular octahedral geometry undoubtedly reflects the steric requirements of the macrocyclic ligand. The 'bite' angles for the 5-membered chelate rings are 81.30(9) and 84.38(6)° while the corresponding angles for the two 6-membered rings are each 89.78(7)°. The Ni–O bond of 2.1214(17) Å slightly exceeds the sum of the covalent radii[28] of octahedral Ni(II) (1.39 Å) and O (0.66 Å) however, it is comparable to the mean literature value of 2.15 Å for this bond type.[29] The Ni–N distances 2.0675(17)–2.1214(17) Å fall within the range (2.03–2.16 Å) observed for such bonds involving neutral sp^3-hybridised nitrogen atoms in macrocyclic high-spin Ni(II) complexes.[30]

The [Ni**L**Cl]$^+$ [**L** = **8** (ON/NON)] cation is characterised by the presence of two chemically identical but crystallographically distinct molecules per unit cell; one molecule is shown in Fig. 6. As for the Ni(II) complex of **7** (ON/NNN), the sixth coordination position is occupied by a chloro ligand. For both molecules the distortion from regular octahedral geometry again largely reflects the small 'bites' of the 5-membered chelate rings [79.61(13)–82.74(15)°], while the 6-membered chelate rings range between 88.17(15)–90.93(15)°. The Ni–N distances and Ni–O bond lengths are again unexceptional.

X-ray structures were also obtained for [Cu**L**Cl_2]·CH_3CN [**L** = **7** (ON/NNN)], [Cu**L**Cl]Cl·2.375H_2O [**L** = **9** (ON/NSN)] and [Cu**L**Cl_2]·CH_3CN [**L** = **8** (ON/NON)]. In both complexes of type [Cu**L**Cl_2] [**L** = **7** (ON/NNN) and **L** = **8** (ON/NON)], the Cu(II) centres are five-coordinate (with the position of the metal ion relative to the macrocyclic cavity differing considerably between the two complexes), while in the complex of **9** (ON/NSN)] the metal ion is six-coordinate. The Cu(II) is coordinated to

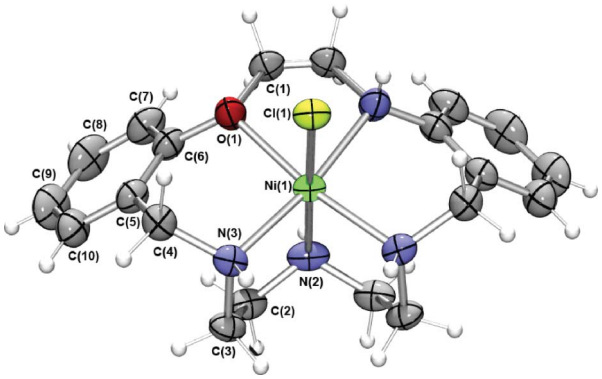

Fig. 5 ORTEP plot of $[NiLCl]^+$ [**L** = **7** (ON/NNN)]; symmetry code used for generating equivalent atoms: x, −y, z. Selected bond lengths (Å) and angles (°): N(3)–Ni(1) 2.0675(17), N(2)–Ni(1) 2.113(2), Cl(1)–Ni(1) 2.4481(7), Ni(1)–O(1) 2.1214(17); N(3)–Ni(1)–N(3) 99.15(10), N(3)–Ni(1)–N(2) 84.38(6), N(3)–Ni(1)–O(1) 89.78(7), N(2)–Ni(1)–O(1) 96.71(7), N(3)–Ni(1)–N(1) 171.07(7), O(1)–Ni(1)–N(1) 81.30(9), N(3)–Ni(1)–Cl(1) 91.85(5), N(2)–Ni(1)–Cl(1) 174.15(7), O(1)–Ni(1)–Cl(1) 87.71(6).

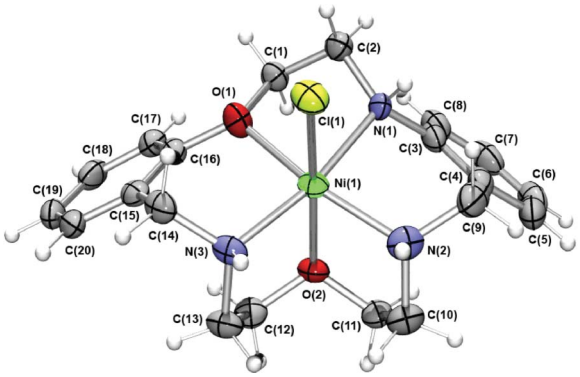

Fig. 6 ORTEP plot of one of the two independent cations of type $[NiLCl]^+$ [**L** = **8** (ON/NON)] present in the unit cell. Selected bond lengths (Å) and angles (°): N(1)–Ni(1) 2.119(3), N(2)–Ni(1) 2.077(4), N(3)–Ni(1) 2.053(4), O(1)–Ni(1) 2.168(4), O(2)–Ni(1) 2.166(3), Cl(1)–Ni(1) 2.4029(11); N(3)–Ni(1)–N(2) 103.17(17), N(3)–Ni(1)–N(1) 168.65(15), N(2)–Ni(1)–N(1) 88.19(15), N(3)–Ni(1)–O(2) 81.79(13), N(2)–Ni(1)–O(2) 82.10(14), N(1)–Ni(1)–O(2) 99.90(12), N(3)–Ni(1)–O(1) 89.15(14), N(2)–Ni(1)–O(1) 165.36(15), N(1)–Ni(1)–O(1) 79.59(13), O(2)–Ni(1)–O(1) 92.04(12), N(3)–Ni(1)–Cl(1) 91.94(10), N(2)–Ni(1)–Cl(1) 94.48(11), N(1)–Ni(1)–Cl(1) 87.25(10), O(2)–Ni(1)–Cl(1) 171.93(9), O(1)–Ni(1)–Cl(1) 92.95(9).

the –NYN– (Y = N, O, S) fragment in all three cases while the aryl ether oxygens and anilino nitrogens remain uncoordinated in the complexes of **5** (ON/NNN) and **8** (ON/NON), but are bound in $[CuLCl]^+$ [**L** = **9** (ON/NSN)].

The coordination sphere of $[CuLCl_2]$ [**L** = **7** (ON/NNN)] (Fig. 7) is comprised of the 1,4,7-triazaheptane macrocyclic fragment and a chloro ligand in an equatorial fashion, while the second chloro ligand occupies an axial position in a distorted square pyramidal coordination geometry (see below). In contrast to the solid state structure of free **7**,[12] the macrocyclic ring is folded in this complex and coordinates in an *exo* manner such that the copper ion is not contained in the macrocyclic cavity. The Cu–N bond distances are unexceptional (mean value 2.0394 Å). Similarly, the Cu–Cl lengths of 2.3003(5) and 2.4705(4) Å fall well within the range (2.11–2.64

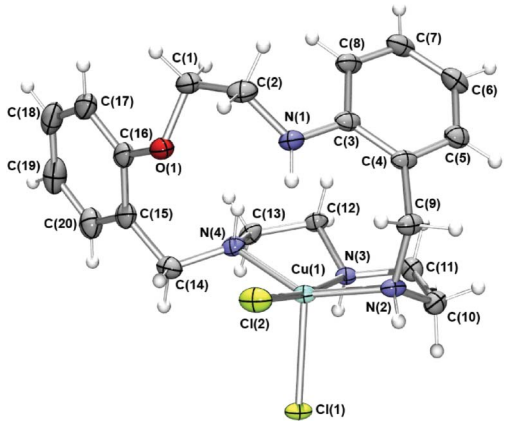

Fig. 7 ORTEP plot of $[CuLCl_2]$ [**L** = **7** (ON/NNN)]. Selected bond lengths (Å) and angles (°): N(2)–Cu(1) 2.0361(15), N(3)–Cu(1) 2.0281(14), N(4)–Cu(1) 2.0540(15), Cl(1)–Cu(1) 2.4705(4), Cl(2)–Cu(1) 2.3003(5); N(3)–Cu(1)–N(2) 84.40(6), N(3)–Cu(1)–N(4) 83.01(6), N(2)–Cu(1)–N(4) 146.91(6), N(3)–Cu(1)–Cl(2) 171.52(4), N(2)–Cu(1)–Cl(2) 93.15(4), N(4)–Cu(1)–Cl(2) 94.84(4), N(3)–Cu(1)–Cl(1) 89.44(4), N(2)–Cu(1)–Cl(1) 101.91(4), N(4)–Cu(1)–Cl(1) 108.43(4), Cl(2)–Cu(1)–Cl(1) 99.015(16).

Å) of values observed for related five-coordinated complexes.[31] The aryl ether oxygen O(1) does not coordinate. This is not unexpected since ether oxygen donors have been documented to be generally 'poor to borderline' donors towards Cu(II); for example, classical crown ethers show little affinity for Cu(II).[32] Similarly, X-ray studies have confirmed the non-coordination of ether functions in copper compounds of mixed oxygen-nitrogen donor macrocycles related to those under discussion.[31,33,34]

Addison's τ parameter[35] can be employed to measure the degree of trigonality present in a five-coordinate complex and is defined as $\tau = (\beta - \alpha)/60°$, where α and β are the largest angles in the coordination sphere. For a perfectly square pyramidal geometry $\tau = 0$, while for a perfectly trigonal-bipyramidal geometry $\tau = 1$. The choice of axial donor is made using the criterion that it should not be any of the four donors which define the two largest angles. A value $\tau = 0.41$ (171.52° − 146.91°)/60° = 0.41) was obtained for $[CuLCl_2]$ (**L** = **7**) which places Cl(1) in the axial coordination site and confirms the distorted square pyramidal assignment for the structure of $[CuLCl_2]$ (**L** = **7** (ON/NNN)].

In contrast to the above structure, the copper centre in $[CuLCl_2]\cdot CH_3CN$ (**L** = **8** (ON/NON)] is contained inside the macrocyclic cavity (Fig. 8), even though the aryl ether oxygen O(1) and the anilino nitrogen N(1) are not bound. The overall coordination geometry is close to square pyramidal ($\tau = 0.04$, α = 158.72°, β = 161.10°) with the equatorial positions being occupied by two chloro ligands and the nitrogen donors of the –NON– fragment, while the ether oxygen O(2) coordinates in the axial position. The bite angles resulting from the formation of the two 5-membered chelate rings are 81.08(5) and 81.16(5) Å). The Cu–N, Cu–O and Cu–Cl distances all fall within their expected ranges.

Finally, the X-ray structure of $[CuLCl]Cl\cdot 2.375H_2O$ [**L** = **9** (ON/NSN)] reveals the presence of two molecules per unit cell, with the macrocycle coordinating *via* all five donor atoms to the central copper. The coordination geometry is distorted octahedral with a chloro ligand occupying the sixth coordination position (Fig. 9). The distortion from regular octahedral geometry is reflected in the observed range of metal–donor bond angles,

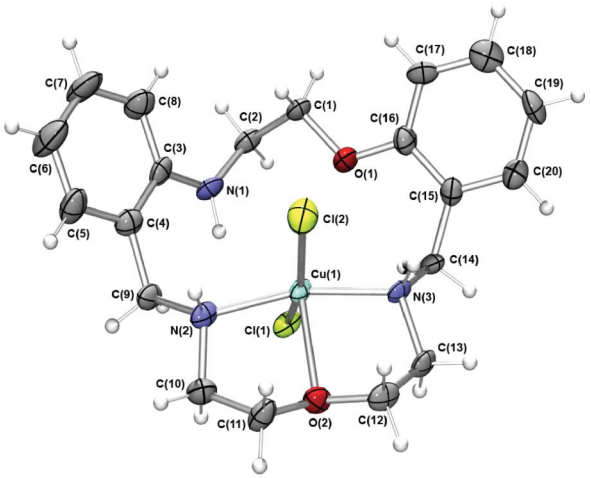

Fig. 8 ORTEP plot of [Cu**L**Cl$_2$] [**L** = **8** (ON/NON)]. Selected bond lengths (Å) and angles (°): N(3)–Cu(1) 2.0510(14), Cl(1)–Cu(1) 2.3019(14), N(2)–Cu(1) 2.0779(14), O(2)–Cu(1) 2.25206(11), Cl(2)–Cu(1) 2.2915(4); N(3)–Cu(1)–N(2) 160.45(6), N(3)–Cu(1)–O(2) 81.08(5), N(2)–Cu(1)–O(2) 81.16(5), N(3)–Cu(1)–Cl(2) 89.87(4), N(2)–Cu(1)–Cl(2) 87.71(4), O(2)–Cu(1)–Cl(2) 107.45(3), N(3)–Cu(1)–Cl(1) 96.08(4), N(2)–Cu(1)–Cl(1) 93.15(4), O(2)–Cu(1)–Cl(1) 93.69(3), Cl(2)–Cu(1)–Cl(1) 158.703(19).

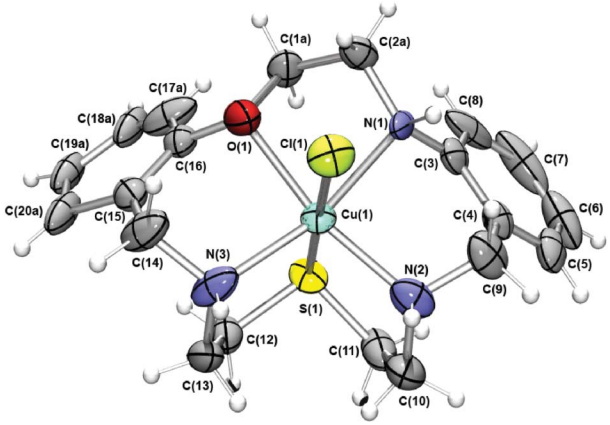

Fig. 9 ORTEP plot of one of the two independent cations of type [Cu**L**Cl]$^+$ [**L** = **9** (ON/NSN)]. Selected bond lengths (Å) and angles (°): N(1A)–Cu(1) 2.333(7), N(2)–Cu(1) 2.090(7), N(3)–Cu(1) 2.133(8), O(1)–Cu(1) 2.235(6), S(1)–Cu(1) 2.365(2), Cl(1)–Cu(1) 2.331(2); N(2)–Cu(1)–N(3) 107.0(3), N(2)–Cu(1)–O(1) 163.9(3), N(3)–Cu(1)–O(1) 87.6(2), N(2)–Cu(1)–Cl(1) 94.2(2), N(3)–Cu(1)–Cl(1) 95.2(2), O(1)–Cu(1)–Cl(1) 91.05(19), N(2)–Cu(1)–N(1A) 88.3(2), N(3)–Cu(1)–N(1A) 162.5(3), O(1)–Cu(1)–N(1A) 76.3(2), Cl(1)–Cu(1)–N(1A) 91.96(18), N(2)–Cu(1)–S(1) 85.2(2), N(3)–Cu(1)–S(1) 85.3(2), O(1)–Cu(1)–S(1) 89.45(19), Cl(1)–Cu(1)–S(1) 179.29(9), N(1A)–Cu(1)–S(1) 87.68(18).

the smallest being the 5-membered chelate rings incorporating the –ON– donor fragment [76.3(2) and 76.8(2)°]. The Cu(2)–O(2) distance is somewhat extended (2.511(5) Å), but lies within the overall range reported for such Cu–O distances (2.11–2.75 Å);[36] its length may reflect the presence of a Jahn–Teller elongation.

Table 3 Protonation constants of the macrocycles **1–9** (I = 0.1; NEt_4ClO_4) (95% methanol, 25 °C)

Ligand	log β_1	log β_2	log β_3
1 (SO/NNN)	9.26	16.90	18.76
2 (SO/NON)	8.67	15.95	—
3 (SO/NSN)	8.29	15.06	—
4 (SN/NNN)	9.44	16.16	18.60
5 (SN/NON)	8.84	16.24	18.84
6 (SN/NSN)	8.37	15.34	18.18
7 (ON/NNN)	9.54	17.49	—
8 (ON/NON)	9.08	16.74	19.52
9 (ON/NSN)	8.76	15.48	17.46

Table 4 Metal stability constants (ML^{n+}) for the macrocycles **1**–**18** (95% methanol, 25 °C)

Ligand (donor sequence)	Co(II)	Ni(II)	Cu(II)
1 (SO/NNN)	7.2	~ 9.3	13.9
2 (SO/NON)	<3.5	<3.5	6.1
3 (SO/NSN)	<3.5	—[a]	7.4
4 (SN/NNN)	—[a]	—[a]	15.6
5 (SN/NON)	3.6	6.1	9.7
6 (SN/NSN)	5.4	7.8	12.4
7 (ON/NNN)	9.2	—[a]	15.6
8 (ON/NON)	4.1	5.5	9.3
9 (ON/NSN)	6.2	7.2	11.2
10 (NN/NNN)	—[a]	—[a]	16.3[b]
11 (NN/NON)	—[a]	—[a]	14.5[b]
12 NN/NSN)	—[a]	—[a]	14.5[b]
13 (OO/NNN)	7.7[c]	10.0[c]	14.4[d]
14 (OO/NON)	<3.5[e]	<3.5[e]	6.5[b]
15 (OO/NSN)	~3.0[e]	5.5[e]	7.4[b]
16 (SS/NNN)	—[a]	9.5[e]	15.6[b]
17 (SS/NON)	<3.5[e]	~3.4[e]	6.9[b]
18 (SS/NSN)	<3.5[e]	<3.5[e]	8.1[b]

[a] Precipitation, hydrolysis or slow approach to equilibrium prevented determination of this log K value. [b] From ref. 36. [c] From ref. 37. [d] From ref. 32. [e] From ref. 38.

Potentiometric titrations

Protonation constants and metal complex stability constants in 95% methanol were determined for **1–9** using the potentiometric (pH) titration technique and, as expected, confirm that each of these ligands is a moderately strong base (Table 3). The corresponding log K values for 1 : 1 complex formation with Co(II), Ni(II) and Cu(II) are given in Table 4 along with those for the closely related mixed donor symmetrical ligands **10–18** whose log K values were reported previously.[33,37–40]

Inspection of the stability data presented in Table 4 (and Fig. 10 and 11) allows the following observations to be made.

(1) Where full data are available, the stabilities for individual metal–ligand systems clearly follow the Irving–Williams stability order of Co(II) < Ni(II) < Cu(II) in all cases.[40]

(2) As anticipated,[37] the magnitude of a particular log K value is strongly influenced by the number of nitrogen donor atoms present in individual ligand systems; with stronger binding for a particular metal occurring as the number of nitrogens increases. For example, on replacing the sulfur in the backbone of **1** (SO/NNN) with a nitrogen to yield **7** (ON/NNN), while maintaining the –NNN– donor fragment unchanged (see Fig. 10), results in the stability of the corresponding Co(II) complex being enhanced by10^2. Similar behaviour is evident on comparing the stabilities of the

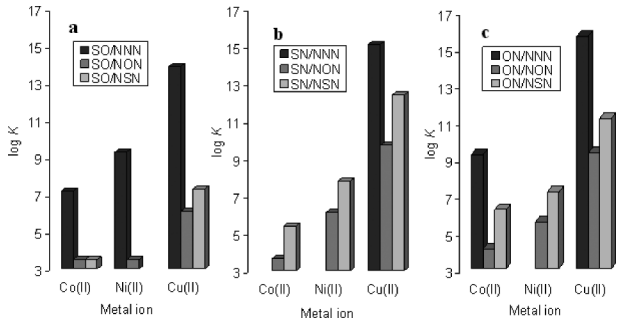

Fig. 10 Comparison of the log *K* values for 1 : 1 (metal : ligand) complexation for the macrocyclic systems incorporating the SO-, SN- and ON-donors in the XZ positions of the macrocyclic rings (see **a**, **b** and **c** respectively).

Ni(II) complexes of **2** (SO/NON) and **5** (SN/NON) where the corresponding log *K* values increase from <3.5 to 6.1. In the case of Cu(II), changing the aryl oxygen in the backbone of **3** (SO/NSN) for nitrogen to yield **6** (SN/NSN) results in the stability of the latter Cu(II) complexes being enhanced by 10^5.

(3) While the dependence of the stability of the metal complexes on the X, Y and Z donors (see Fig.10 and 11) is clearly more complex, the results do confirm the expected[41–45] low affinity of ether oxygen donors for the above transition metal ions, with in most instances the affinity of thioether sulfur being somewhat higher than ether oxygen for these metals. Thus, for example, replacement of oxygen donors by sulfur results in a modest increase in the stability of the complexes of **6** (SN/NSN) and **9** (ON/NSN) compared to those of **5** (SN/NON) and **8** (ON/NON) respectively. In this context, it is noted that a small preference of Cu(II) for thioether sulfur over ether oxygen has been reported previously.[41,46,47]

(4) As discussed earlier, the X-ray structures of the crystalline Cu(II) complexes of both **7** (ON/NNN) and **8** (ON/NON) both show that macrocycle coordination only occurs *via* the respective –NYN– fragments. Hence if similar behaviour predominates in solution then the observed magnitudes of the binding strengths of these ligands for Cu(II) likely simply reflect the different affinities of the respective –NNN- and –NON- fragments of each macrocycle for this metal ion.

(5) The data presented in Fig. 11 also confirm that varying the order of the donor atom sequence in the macrocyclic backbone can have a significant effect on the stability of individual complexes. For example, varying the O_2N_3S-donor sequence from ON/NSN in **9** to SN/NON in **5** results in a drop in the log *K* values for the corresponding Co(II) complexes from 6.2 to 3.6. Similarly the donor sequence of OO/NNN in **13** gives a log *K* value for Ni(II) of 10.0 while the sequence of ON/NON in **8** results in a drop in the corresponding log *K* value to 5.5 (however, in this case the observed reduction may also be contributed to by the presence in **8** of a less basic anilino amine together with two secondary aliphatic amines against three secondary aliphatic amines present in **13**).

Concluding remarks

Investigation of the effect of variation of both donor atom type and donor atom sequence across eighteen 17-membered macrocyclic ligands incorporating both symmetrical and unsymmetrical N, S and/or O donors has enabled a comparative structure/function analysis of their metal binding properties towards Co(II), Ni(II) and Cu(II). To the best of our knowledge this number of macrocyclic rings (involving similar ring size and backbone structure) is unprecedented in terms of previously reported comparative studies of the present type. The results both confirm previous observations concerning the influence of the nature of the donor atom set on complexation behaviour as well as providing additional information that, collectively, provides a basis for the rational design of new related macrocyclic ligand systems exhibiting predetermined metal binding properties – including, for example, systems involving other ring sizes and/or backbone structures.

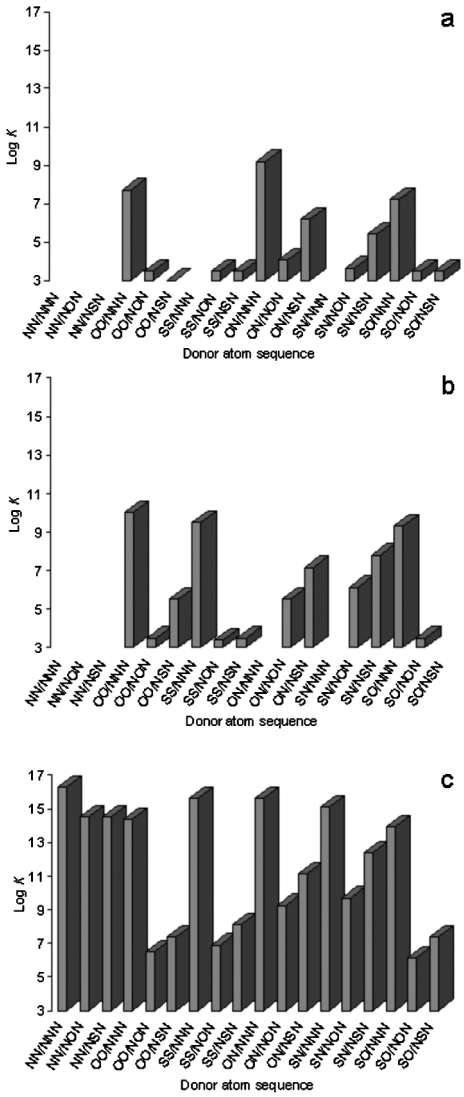

Fig. 11 Log *K* values for the (a) Co(II), (b) Ni(II) and (c) Cu(II) complexes of the related five-donor, 17-membered macrocycles shown. In these figures the absence of bars indicate that no experimental data was obtained; log values recorded as <3.5 in Table 4 are shown at their maximum value of 3.5.

Acknowledgements

We thank the Australian Research Council for support.

References

1 A. Trujillo, M. Fuentealba, D. Carrillo, C. Manzur, I. Ledoux-Rak, J.-R. Hamon and J.-Y. Saillard, *Inorg. Chem.*, 2010, **49**, 2750.
2 S. Akine, A. Akimoto, T. Shiga, H. Oshio and T. Nabeshima, *Inorg. Chem.*, 2008, **47**, 875.
3 D. Pawlica, M. Marszałek, G. Mynarczuk, L. Sieroń and J. Eilmes, *New J. Chem.*, 2004, **28**, 1615.
4 R. Pasche, D. Balkow and E. Sinn, *Inorg. Chem.*, 2002, **41**, 1949; B. Shi, M. Scobie and R. W. Boyle, *Tetrahedron Lett.*, 2003, **44**, 5083.
5 A. Kuik, Z. Szarka, R. Skoda-Foldes and L. Kollar, *Lett. Org. Chem.*, 2004, **1**, 151.
6 K.-H. Park, *J. Org. Chem.*, 2005, **70**, 2075.
7 N. T. S. Phan, D. H. Brown, H. Adams, S. E. Spey and P. Styring, *Dalton Trans.*, 2004, 1348.
8 A. Iwan and H. Janeczek, *Mol. Cryst. Liq. Cryst.*, 2010, **518**, 101.
9 L. F. Lindoy, G. V. Meehan, I. M. Vasilescu, H. J. Kim, J.-E. Lee and S. S. Lee, *Coord. Chem. Rev.*, 2010, **254**, 1713.
10 I. M. Vasilescu, D. J. Bray, J. K. Clegg, L. F. Lindoy, G. V. Meehan and G. Wei, *Dalton Trans.*, 2006, 5115; M. Feinerman-Melnikova, A. Nezhadali, G. Rounaghi, J. C. McMurtrie, J. Kim, K. Gloe, M. Langer, S. S. Lee, L. F. Lindoy, T. Nishimura, K.-M. Park and J. Seo, *Dalton Trans.*, 2004, 122; K. J. Park, J.-H. Kim, G. V. Meehan, T. Nishimura, L. F. Lindoy, S. S. Lee, K.-M. Park and I. Yoon, *Aust. J. Chem.*, 2002, **55**, 773; L. F. Lindoy, *Coord. Chem. Rev.*, 1998, **174**, 327; K. R. Adam, D. S. Baldwin, P. A. Duckworth, L. F. Lindoy, M. McPartlin, A. Bashall, H. R. Powell and P. A. Tasker, *J. Chem. Soc., Dalton Trans.*, 1995, 1127; L. F. Lindoy, *Pure Appl. Chem.*, 1989, **61**, 1575; K. D. S. Baldwin, P. A. Duckworth, G. R. Erickson, L. F. Lindoy, M. McPartlin, G. M. Mockler, W. E. Moody and P. A. Tasker, *Aust. J. Chem.*, 1987, **40**, 1861; K. R. Adam, G. Anderegg, K. Henrick, A. J. Leong, L. F. Lindoy, H. C. Lip, M. McPartlin, R. J. Smith and P. A. Tasker, *Inorg. Chem.*, 1981, **20**, 4048.
11 M. J. Bjerrum, T. Lailer and E. Larsen, *Inorg. Chem.*, 1986, **25**, 816.
12 D. S. Baldwin, B. F. Bowden, P. A. Duckworth, L. F. Lindoy, B. J. McCool, G. V. Meehan, I. M. Vasilescu and S. B. Wild, *Aust. J. Chem.*, 2002, **55**, 597.
13 H. J. Kim, A. J. Leong, L. F. Lindoy, J. Kim, J. Nachbaur, A. Nezhadali, G. Rounaghi and G. Wei, *J. Chem. Soc., Dalton Trans.*, 2000, 3453 and references therein.
14 P. Gans, A. Sabatini and A. Vacca, *Inorg. Chim. Acta*, 1976, **18**, 237.
15 Bruker-Nonius (2003). *APEX v2.1, SAINT v.7 and XPREP v.6.14*, Bruker AXS Inc. Madison, Wisconsin, USA.
16 Bruker (1995), *SMART, SAINT and XPREP*. Bruker Analytical X-ray Instruments Inc., Madison, Wisconsin, USA.
17 L. J. Farrugia, *J. Appl. Crystallogr.*, 1999, **32**, 837.
18 A. Altomare, M. C. Burla, M. Camalli, G. L. Cascarano, C. Giocavazzo, A. Guagliardi, A. G. C. Moliterni, G. Polidori and S. Spagna, *J. Appl. Crystallogr.*, 1999, **32**, 115.
19 G. M. Sheldrick, in *Empirical Absorption and Correction Software*, University of Goettingen, Germany, 1999–2007.
20 G. M. Sheldrick, in *Programs for Crystal Structure Analysis*, University of Goettingen, Germany, 1997.
21 L. F. Lindoy, S. Mahendran, K. E. Krakowiak, H. An and J. S. Bradshaw, *J. Heterocycl. Chem.*, 1992, **29**, 141; M. Menif, A. E. Martell, P. J. Squattrito and A. Clearfield, *Inorg. Chem.*, 1990, **29**, 4723; M. Pietraszkiewicz and R. Gasiorowski, *Chem. Ber.*, 1990, **123**, 405.
22 R. M. Silverstein, F. X. Webster and D. J. Kiemle, *Spectrometric Identification of Organic Compounds*, 7th edn, John Wiley and Sons Inc., New York, 2005.
23 J. Suresh, R. S. Kumar, S. Perumal and S. Natarajan, *Acta Crystallogr., Sect. E: Struct. Rep. Online*, 2007, **63**, o777; M. Du, X.-J. Jiang and X.-J. Zhao, *Acta Crystallogr., Sect. E: Struct. Rep. Online*, 2005, **61**, m485; L. F. Lindoy and I. M. Atkinson, *Self-assembly in Supramolecular Chemistry. Royal Society for Chemistry*, Cambridge UK, 2000.
24 J. W. Steed and J. L. Atwood, *Supramolecular Chemistry*, 2nd edn, John Wiley and Sons Ltd, 2009, Chichester, UK, pp. 517–518.
25 K. R. Adam, L. G. Brigden, K. Henrick, L. F. Lindoy, M. McPartlin, B. Mimnagh and P. A. Tasker, *J. Chem. Soc., Chem. Commun.*, 1985, 710.
26 U. Kallert and R. Mattes, *Inorg. Chim. Acta*, 1991, **180**, 263.
27 U. Kallert and R. Mattes, *Polyhedron*, 1992, **11**, 617.
28 L. Pauling, *The Nature of the Chemical Bond*, 3rd edn, Cornell University Press, Ithaca, NY, 1960.
29 H. J. Goodwin, K. Henrick, L. F. Lindoy, M. McPartlin and P. A. Tasker, *Inorg. Chem.*, 1982, 3261 and references therein.
30 A. Ekstrom, L. F. Lindoy, H. C. Lip, R. J. Smith, H. J. Goodwin, M. McPartlin and P. A. Tasker, *J. Chem. Soc., Dalton Trans.*, 1979, 1027 and references therein.
31 K. R. Adam, G. Anderegg, L. F. Lindoy, H. C. Lip, M. McPartlin, J. H. Rea, R. J. Smith and P. A. Tasker, *Inorg. Chem.*, 1980, **19**, 2959 and references therein.
32 L. F. Lindoy, *The Chemistry of Macrocyclic Ligand Complexes*, Cambridge University Press, Cambridge, 1989.
33 K. R. Adam, L. F. Lindoy, H. C. Lip, J. H. Rea, B. W. Skelton and A. H. White, *J. Chem. Soc., Dalton Trans.*, 1981, 74.
34 J. Seo, S. Park, S. S. Lee, M. Feinerman-Melnikova and L. F. Lindoy, *Inorg. Chem.*, 2009, **48**, 2770.
35 A. W. Addison, T. N. Rao, J. Reedijk, J. van Rijn and G. C. Verschoor, *J. Chem. Soc., Dalton Trans.*, 1984, 1349.
36 N. A. Bailey, D. E. Fenton, S. J. Kitchen, T. H. Lilley, M. G. Williams, P. A. Tasker, A. J. Leong and L. F. Lindoy, *J. Chem. Soc., Dalton Trans.*, 1991, 627 and references therein.
37 K. R. Adam, D. S. Baldwin, P. A. Duckworth, A. J. Leong, L. F. Lindoy, M. McPartlin and P. A. Tasker, *J. Chem. Soc., Chem. Commun.*, 1987, 1124.
38 K. R. Adam, A. J. Leong, L. F. Lindoy, H. C. Lip, B. W. Skelton and A. H. White, *J. Am. Chem. Soc.*, 1983, **105**, 4645.
39 K. R. Adam, M. Antolovich, D. S. Baldwin, L. G. Brigden, P. A. Duckworth, L. F. Lindoy, A. Bashall, M. McPartlin and P. A. Tasker, *J. Chem. Soc., Dalton Trans.*, 1992, 1869.
40 H. Irving and R. J. P. Williams, *J. Chem. Soc.*, 1953, 3192.
41 R. M. Izatt, J. S. Bradshaw, S. A. Nielsen, J. D. Lamb, J. J. Christensen and D. Sen, *Chem. Rev.*, 1985, **85**, 271.
42 R. M. Izatt, K. Pawlak, J. S. Bradshaw and R. L. Bruening, *Chem. Rev.*, 1991, **91**, 1721.
43 R. M. Izatt, K. Pawlak and J. S. Bradshaw, *Chem. Rev.*, 1995, **95**, 2529.
44 G. Reid and M. Schroder, *Chem. Soc. Rev.*, 1990, **19**, 239.
45 A. J. Blake and M. Schroder, *Adv. Inorg. Chem.*, 1990, **35**, 1.
46 J.-H. Kim, M.-H. Cho, D.-H. Hyeoun, H. B. Park, S. J. Kim and I.-C. Lee, *J. Korean Chem. Soc.*, 1990, **34**, 418.
47 K. R. Adam, M. Antolovich, D. S. Baldwin, P. A. Duckworth, A. J. Leong, L. F. Lindoy, M. McPartlin and P. A. Tasker, *J. Chem. Soc., Dalton Trans.*, 1993, 1013.

